Identification of Potential Regulatory Sites of the Na^+,K^+-ATPase by Kinetic Analysis†

Benjamin Y. Kong and Ronald J. Clarke*

School of Chemistry, University of Sydney, Sydney, New South Wales 2006, Australia

Received August 28, 2003; Revised Manuscript Received December 22, 2003

ABSTRACT: Kinetic models are presented that allow the Na^+,K^+-ATPase steady-state turnover number to be estimated at given intra- and extracellular concentrations of Na^+, K^+, and ATP. Based on experimental transient kinetic data, the models utilize either three or four steps of the Albers−Post scheme, that is, $E_2 \rightarrow E_1$, $E_1 \rightarrow E_2P$ (or $E_1 \rightarrow E_1P$ and $E_1P \rightarrow E_2P$), and $E_2P \rightarrow E_2$, which are the major rate-determining steps of the enzyme cycle. On the time scale of these reactions, the faster binding steps of Na^+, K^+, and ATP to the enzyme are considered to be in equilibrium. Each model was tested by comparing calculations of the steady-state turnover from rate constants and equilibrium constants for the individual partial reactions with published experimental data of the steady-state activity at varying Na^+ and K^+ concentrations. To provide reasonable agreement between the calculations and the experimental data, it was found that Na^+/K^+ competition for cytoplasmic binding sites was an essential feature required in the model. The activity was also very dependent on the degree of K^+-induced stimulation of the reverse reaction $E_1 \rightarrow E_2$. Taking into account the physiological substrate concentrations, the models allow the most likely potential sites of short-term Na^+,K^+-ATPase regulation to be identified. These were found to be (a) the cytoplasmic Na^+ and K^+ binding sites, via changes in Na^+ or K^+ concentration or their dissociation constants, (b) ATP phosphorylation (as a substrate), via a change in its rate constant, and (c) the position of the $E_2 \rightleftharpoons E_1$ equilibrium.

The Na^+,K^+-ATPase[1] was the first ion pump to be discovered (*1*), and it is one of the most fundamentally important enzymes of animal physiology. The electrochemical potential gradient for Na^+ ions, which the enzyme maintains, is used as the driving force for numerous secondary transport systems. Examples include the Na^+ channels in nerve, which allow the action potential to be produced, the Na^+−glucose cotransporter, which is responsible for glucose uptake in cells, and the Na^+/Ca^{2+} exchanger in heart, which plays an important role in muscle relaxation. The Na^+,K^+-ATPase, furthermore, contributes to the osmotic regulation of cell volume and is a major determinant of body temperature. Because of these many important functions, its activity in the cell must be under tight metabolic control. Before one can begin to understand the mechanisms of Na^+,K^+-ATPase regulation, however, the mechanism and the kinetics of the enzyme's complex reaction cycle must be understood.

The sequence of reaction steps that the Na^+,K^+-ATPase undergoes and the stoichiometry of its substrates are now well established (*2*). They are generally described by the Albers−Post scheme, which describes a cyclic sequential mechanism comprising cytoplasmic Na^+ and ATP binding, phosphorylation, a conformational change of the phosphorylated enzyme, extracellular Na^+ release and K^+ binding, dephosphorylation, a conformational change of the unphosphorylated enzyme, and finally cytoplasmic K^+ release. Over the years, many groups have been involved in the determination of rate constants and equilibrium constants for the individual reaction steps of the cycle. The first complete kinetic model of the whole reaction cycle, which allowed simulations of steady-state activity and transient experiments, was published by Heyse et al. (*3*). The model used an expanded Albers−Post scheme containing 32 different rate constants and 2 equilibrium constants, and the simulations were performed by the numerical integration of 15 separate differential rate equations. The aim of Heyse et al. (*3*) and subsequent work by the same group (*4*) was to dissect the Albers−Post cycle to try to identify a reaction acting as a power stroke, in which the energy of ATP hydrolysis is released to drive ion transport.

The present paper also involves simulations of Na^+,K^+-ATPase steady-state activity, but its aim is very different. Here we shall describe the identification of possible regulatory mechanisms of the enzyme based on a consideration of the kinetics of its partial reactions. For this purpose we are of the opinion that it is not necessary to consider the kinetics of every individual reaction of the Albers−Post cycle but only the rate-determining steps, since only the rates of these steps determine the overall turnover number of the enzyme cycle. Apart from the difference in the aim of the work and the approach to kinetic modeling, the kinetic models presented here also contain revised values of some of the most important rate constants. Of major importance is the correct identification of the rate-determining steps of the

† This work was supported by an Australian Research Council Discovery Grant DP0208282 (to R.J.C).

* To whom correspondence should be addressed. Phone: +61 2 9351 4406. Fax: +61 2 9351 3329. E-mail: r.clarke@chem.usyd.edu.au.

[1] Abbreviations: Na^+,K^+-ATPase, sodium and potassium ion-activated adenosine triphosphatase; ATP, adenosine 5′-triphosphate; ADP, adenosine 5′-diphosphate; E_1, E_2, E_1P, and E_2P, intermediates of the Na^+,K^+-ATPase pump cycle; RH421, *N*-(4-sulfobutyl)-4-(4-(*p*-(dipentylamino)phenyl)butadienyl)-pyridinium inner salt.

10.1021/bi0355443 CCC: $27.50
Published on Web 02/05/2004

enzyme cycle, which are most likely to be involved in physiological regulation. According to the model of Heyse et al. (*3*), both the conformational change of unphosphorylated enzyme ($E_2 \rightarrow E_1$) and that of the phosphorylated enzyme ($E_1P \rightarrow E_2P$) have rate constants of 22 s^{-1} at saturating ATP concentrations and 20 °C. There is, however, now convincing evidence that the $E_2 \rightarrow E_1$ transition is the major rate-determining step of the entire enzyme cycle (*5*) and that the $E_1P \rightarrow E_2P$ transition is an order of magnitude or more faster than Heyse et al.'s value of 22 s^{-1} (*6*). Because of this error in the assignment of the rate-determining steps, no reliable conclusions on the mechanisms of regulation of the Na^+,K^+-ATPase can be reached on the basis of the model of Heyse et al. (*3*).

To obtain a reliable set of rate constants and thus to identify its most important rate-determining steps, over several years we have been investigating the kinetics of the individual partial reactions of the enzyme. The majority of the experiments were performed on purified Na^+,K^+-ATPase membrane fragments using the stopped-flow technique in combination with the voltage-sensitive probe RH421, but the results were also compared with independent measurements using other techniques, for example, quenched-flow, ATP concentration jump after photolysis of caged-ATP, and frequency-dependent capacitance measurements (*5*−*12*). Now that the most important rate-determining steps have been isolated and their rate constants determined, this allows us to simplify the Albers−Post scheme by considering differential rate equations for the rate-determining steps alone. All other steps can be considered in equilibrium on the time-scale of the rate-determining steps. In an earlier paper (*5*), we published a preliminary model, which did not include substrate dependence of the observed rate constants and was hence only applicable at saturating substrate concentrations. Here we describe more complete models, which include substrate concentrations and, furthermore, distinguish between extra- and intracellular concentrations. One of the models has recently been successfully applied to the analysis of steady-state whole-cell patch-clamp data, and the interpretation of the results obtained in terms of the enzyme's partial reactions (*13*). Here we shall describe the complete models and the assumptions involved and demonstrate their application in simulating steady-state enzyme activity. Based on comparisons between the simulations and experimental activity data, likely mechanisms of enzyme regulation will be identified.

METHODS

Computer simulations of the protein's steady-state hydrolytic activity were performed using the commercially available program Berkeley Madonna 7.0 via the variable step size Rosenbrock integration method for stiff systems of differential equations. The simulations yield the time course of the concentration of each enzyme intermediate, as well as the concentration of inorganic phosphate. On normalization to unitary enzyme concentration, the rate of phosphate production is equivalent to the enzyme's steady-state turnover number. If required, the turnover number can then easily be converted into a steady-state activity (in mol of P_i/g of protein/s) by dividing by the molecular weight of an $\alpha\beta$ unit of the Na^+,K^+-ATPase of 147 000 g mol^{-1} (*14*).

Kinetic Modeling

On the basis of numerous kinetic studies by ourselves and others, three major rate-determining steps of the Na^+,K^+-ATPase have been isolated: (a) the conformational change of unphosphorylated enzyme, $E_2 \rightarrow E_1$ (k_1), (b) the phosphorylation reaction, $E_1 \rightarrow E_1P$ (k_2), and (c) the dephosphorylation reaction, $E_2P \rightarrow E_2$ (k_4). Let us consider first the phosphorylation and dephosphorylation reactions. The phosphorylation reaction requires the presence of intracellular Na^+ ions and ATP and thus plays a particularly important part in rate determination at low intracellular Na^+ or ATP concentrations. The dephosphorylation reaction is induced by extracellular K^+ ions and is hence the major rate-determining step at low extracellular K^+ ions and in the Na^+/Na^+ exchange mode of the enzyme (*15*, *16*). If all substrates are present at saturating concentrations, the major rate-determining step of the reaction cycle is the conformational transition of unphosphorylated enyzme, $E_2 \rightarrow E_1$, which is responsible for the release of bound K^+ ions to the intracellular fluid. This reaction, although it does not necessarily require any substrates, has been found to be accelerated by intracellular ATP (*7*, *9*, *17*−*19*) and extracellular Na^+ (or ionic strength in general) (*12*, *20*−*22*). The conformational transition of phosphorylated enzyme, $E_1P \rightarrow E_2P$ (k_3), has been found to be very fast and to occur immediately following phosphorylation without requiring any additional substrates (*6*). It is, thus, not a major rate-determining step of the enzyme cycle. Nevertheless, at high extracellular Na^+ concentrations, stimulation of the reverse reaction ($E_2P \rightarrow E_1P$) could contribute to an overall drop in turnover (*23*). All other reactions of the enzyme, that is, ion binding and release reactions as well as ATP binding, ADP release, and inorganic phosphate release, are assumed to be in equilibrium on the time scale of the three rate-determining reactions above.

Rather than start modeling with a fully expanded Albers−Post scheme including all possible reactions the enzyme can undergo, we have applied the principle of Occam's razor and reduced the scheme to its bare minimum by considering initially the above three rate-determining steps alone with all substrate binding steps as equilibria. We have then extended the model where necessary by taking into account more transient experimental data to obtain better agreement with the enzyme's steady-state behavior. Apart from being logically sound, this approach has the advantage that it enables one in the process to identify important features in the enzyme's mechanism that play a role in determining its behavior under physiological conditions.

Model 1: Complete Irreversibility, No Competition. In the first instance, all reactions are assumed to be irreversible, and no competition between substrates is considered. The basic scheme (model 1) is shown in Figure 1. To test the success of each model, we have chosen to compare values of the turnover number obtained from the simulations to published experimental data on the steady-state activity of the enzyme at a constant ionic strength of 150 mM but at varying ratios of Na^+ to K^+ ions. This type of experiment was first performed by Skou (*24*) using enzyme isolated from both rabbit brain and kidney. He subsequently extended these studies to investigate the effects of varying ATP concentration and pH, using enzyme isolated from ox brain (*25*, *26*).

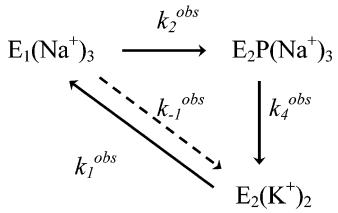

FIGURE 1: Simplified reaction scheme of the Na^+,K^+-ATPase showing only those reactions considered to be rate-determining. Model 1 considers all reactions shown with solid arrows only. Model 2 considers all reactions shown with solid arrows and includes competition between Na^+ and K^+ for two cytoplasmic binding sites on E_1. Model 3 is a further extension of model 2 including K^+-stimulated conversion of E_1 to E_2, indicated by the dashed arrow. Please note that, for simplicity, ATP has not been explicitly included in the reaction scheme. ATP is, however, naturally required for the phosphorylation step ($E_1(Na^+)_3 \rightarrow E_2P\text{-}(Na^+)_3$), and it can also act on a low-affinity site to accelerate the $E_2(K^+)_2 \rightarrow E_1(Na^+)_3$ transition.

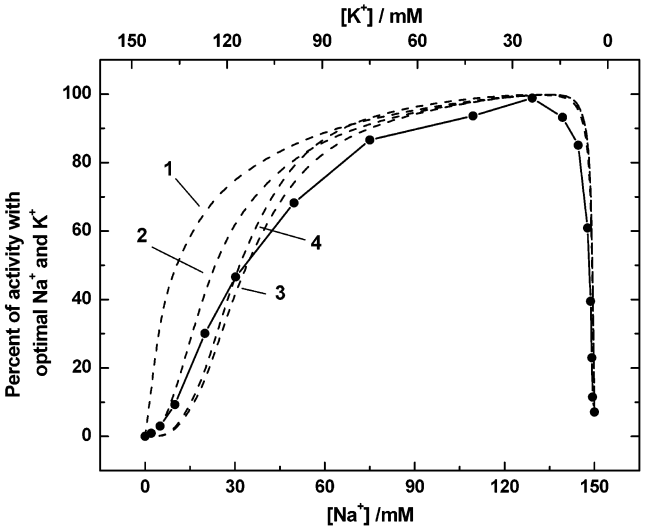

FIGURE 2: Effect of Na^+ and K^+ ($Na^+ + K^+ = 150$ mM) on the catalytic activity of the Na^+,K^+-ATPase. The data (solid line) have been reproduced from Skou (*25*) (●, pH 7.4, 37 °C, [ATP] = 3 mM). Also shown are the results of computer simulations using kinetic models 1−4 (dashed lines). The sums of the squares of the residuals between the experimental and simulated data points were 10 168 (model 1), 5519 (model 2), 5280 (model 3), and 4256 (model 4). For each curve the 100% of optimum activity values correspond to turnover numbers of 37.8 s^{-1} (model 1−3) and 30.9 s^{-1} (model 4).

Skou's data have been reproduced in Figure 2. The major features of his data, which should be noted when comparing to the results of the simulations, are significant drops in activity at high Na^+ concentrations and low K^+ concentrations and a sigmoidal increase in activity at low Na^+ concentrations and high K^+ concentrations. Because of the characteristic shape of the curve, it is often referred to as Skou's "Napoleon hat" experiment.

The aim of the modeling presented here is to describe the overall shape of the activity data using the simplest possible kinetic model and without changing any of the values of the rate constants or equilibrium constants determined directly from studies of the partial reactions. That is, no fitting of the model to Skou's data has been carried out, since this would allow almost any reasonable model to agree with the data. Exact agreement between the simulated data and Skou's experimental data would, however, not be expected for two reasons. First of all, Skou used enzyme from ox brain, which is known to contain a mixture of α_1, α_2, and α_3 isozymes of the enzyme, whereas the experimental data on the partial reactions used for the simulations were measured predominantly on enzyme isolated from rabbit kidney, which is thought to consist predominantly of the α_1 isozyme (*27*). Second, the temperatures at which the steady-state and transient experiments were carried out were different. Skou performed his experiment at 37 °C, whereas the majority of the measurements on the partial reactions were carried out at 24 °C. This difference in temperature might be expected to change the relative values of the various rate constants of the pump cycle, particularly if they have very different activation energies, and this could affect the shape of the activity curve. Such considerations could, thus, easily account for any relatively small deviations between Skou's data and the simulated values of steady-state activity.

The differential rate equations describing model 1 are as follows:

$$\frac{d[E_1]}{dt} = k_1^{obs}[E_2] - k_2^{obs}[E_1] \quad (1)$$

$$\frac{d[E_2P]}{dt} = k_2^{obs}[E_1] - k_4^{obs}[E_2P] \quad (2)$$

$$\frac{d[E_2]}{dt} = k_4^{obs}[E_2P] - k_1^{obs}[E_2] \quad (3)$$

$$\frac{d[P_i]}{dt} = k_4^{obs}[E_2P] \quad (4)$$

All of the rate constants given in eqs 1−4 are termed *observed* rate constants, since they are actually pseudo-first-order rate constants, which only reach their maximum values when all the appropriate substrate concentrations are saturating. The observed rate constants are thus functions of the concentrations of the relevant substrates. The exact form of each function can be derived by applying the theory of relaxation kinetics (*28*−*31*) as described in earlier publications (*7*, *8*, *12*).

The expressions relating the observed rate constants to the substrate concentrations are as follows:

$$k_1^{obs} = \frac{k_1^a + k_1^b[Na^+]_o/K_N^o + k_1^c[ATP]/K_A + k_1^d[Na^+]_o[ATP]/(K_N^o K_A)}{(1 + [Na^+]_o/K_N^o)(1 + [ATP]/K_A)} \quad (5)$$

$$k_2^{obs} = k_2 \frac{[ATP]/K'_A}{1 + [ATP]/K'_A} \times \frac{[Na^+]_i^3/(K_{N1}^2 K_{N2})}{1 + \frac{2[Na^+]_i}{K_{N1}} + \frac{[Na^+]_i^2}{K_{N1}^2} + \frac{[Na^+]_i^3}{(K_{N1}^2 K_{N2})}} \quad (6)$$

$$k_4^{obs} = \frac{k_4^a(1 + [K^+]_o/K_{K1}^o) + k_4^b[K^+]_o^2/(K_{K1}^o K_{K2}^o)}{1 + [K^+]_o/K_{K1}^o + [K^+]_o^2/(K_{K1}^o K_{K2}^o)} \quad (7)$$

Table 1: Values of the Rate and Equilibrium Constants Used for the Simulations

parameter	reaction	value	ref[a]
k_1^a	$E_2 \rightarrow E_1$, $E_2K^+ \rightarrow E_1 + K^+$, and $E_2(K^+)_2 \rightarrow E_1 + 2K^+$[b]	2.3×10^{-2} s^{-1}	*60*
k_1^b	$E_2Na^+ \rightarrow E_1Na^+$, $E_2Na^+K^+ \rightarrow E_1Na^+ + K^+$, and $E_2Na^+(K^+)_2 \rightarrow E_1Na^+ + 2K^+$[b]	0.8 s^{-1}	*9*
k_1^c	$E_2ATP \rightarrow E_1ATP$, $E_2K^+ATP \rightarrow E_1ATP + K^+$, and $E_2(K^+)_2ATP \rightarrow E_1ATP + 2K^+$[b]	11 s^{-1}	*12*
k_1^d	$E_2Na^+ATP \rightarrow E_1Na^+ATP$, $E_2Na^+K^+ATP \rightarrow E_1Na^+ATP + K^+$, and $E_2Na^+(K^+)_2ATP \rightarrow E_1Na^+ATP + 2K^+$[b]	70 s^{-1}	*5*
k_{-1}^a	$E_1 \rightarrow E_2$, $E_1Na^+ \rightarrow E_2Na^+$, $E_1(Na^+)_2 \rightarrow E_2(Na^+)_2$, $E_1(Na^+)_3 \rightarrow E_2(Na^+)_3$, $E_1Na^+K^+ \rightarrow E_2Na^+K^+$, and $E_1K^+ \rightarrow E_2K^+$[c]	5.9×10^{-2} s^{-1}	*60*
k_{-1}^b	$E_1(K^+)_2 \rightarrow E_2(K^+)_2$	550 s^{-1}	*45*
k_2	$E_1(Na^+)_3ATP \rightarrow E_2P + 3Na^+ + ADP$	180 s^{-1}	*7*
k_3	$E_1P(Na^+)_3 \rightarrow E_2P(Na^+)_3$	225 s^{-1}	*46*
k_{-3}	$E_2P(Na^+)_3 \rightarrow E_1P(Na^+)_3$	401 s^{-1}	*46*
k_4^a	$E_2P \rightarrow E_2$ and $E_2PK^+ \rightarrow E_2K^+$	4 s^{-1}	*8, 61*
k_4^b	$E_2P(K^+)_2 \rightarrow E_2(K^+)_2$	312 s^{-1} [d]	*8*
K_A	$E_2ATP \rightleftharpoons E_2 + ATP$ and $E_2Na^+ATP \rightleftharpoons E_2Na^+ + ATP$ [b]	71 μM	*9*
K'_A	$E_1ATP \rightleftharpoons E_1 + ATP$ and $E_1Na^+ATP \rightleftharpoons E_1Na^+ + ATP$ [b]	8.0 μM	*9*
K_N^o	$E_2Na^+ \rightleftharpoons E_2 + Na^+$, and $E_2Na^+ATP \rightleftharpoons E_2ATP + Na^+$ [b]	31 mM	*12*
K_{N1}	microscopic dissociation constant for the first 2 Na^+ ions to E_1	8 mM	*9*
K_{N2}	$E_1(Na^+)_3 \rightleftharpoons E_1(Na^+)_2 + Na^+$ and $E_1(Na^+)_3ATP \rightleftharpoons E_1(Na^+)_2ATP + Na^+$	1.8 mM	*9*
K_{NP}^o	$E_2P(Na^+)_2 \rightleftharpoons E_2P + 2Na^+$	400 mM	*46*
K_{K1}^o	$E_2PK^+ \rightleftharpoons E_2P + K^+$	8 mM	*8*
K_{K2}^o	$E_2P(K^+)_2 \rightleftharpoons E_2PK^+ + K^+$	0.6 mM	*8*
K_K^i	microscopic dissociation constant for the first 2 K^+ ions to E_1	10 mM	*62*

[a] The temperatures utilized in the each of the studies cited were 24 °C (*5*, *7*, *8*, *9*, *12*), 21 °C (*60*, *61*), 25 °C (*45*), and 37 °C (*62*). [b] In each of these reactions, K^+ release is assumed to occur immediately following the conformational change if K^+ ions were initially bound (*9*). The bound Na^+ ions in the case of these reactions refers to extracellularly bound Na^+ on allosteric sites not transport sites (*12*). Mg^{2+} also appears to have a small accelerating effect on this reaction. [c] The measurements of Bugnon et al. (*45*) indicate that the binding of two K^+ is necessary to observe a dramatic increase in the rate constant of the $E_1 \rightarrow E_2$ transition. Therefore, although the value of 0.06 s^{-1} measured by Apell et al. (*60*) actually refers to conditions in the absence of both Na^+ and K^+ ions, we have made the assumption that the same value applies when up to three Na^+ ions are bound, one K^+ ion is bound, or one K^+ and one Na^+ ion are bound. [d] Kane et al. (*8*) measured experimentally the sum of the rate constants for K^+-stimulated dephosphorylation plus rephosphorylation via ATP to be 366 s^{-1}. The rate constant for K^+-stimulated dephosphorylation has, therefore, been estimated by subtracting the rate constant for the transition, $E_2Na^+ATP \rightarrow E_1Na^+ATP$ (the rate-determining step for rephosphorylation), of 54 s^{-1} from this value.

Equations 5, 6, and 7 have been adapted from Humphrey et al. (*12*), Kane et al. (*7*), and Kane et al. (*8*), respectively, by excluding all terms relating to backward reactions and converting all association constants into dissociation constants. $[Na^+]_o$ and $[K^+]_o$ refer to the extracellular concentrations of Na^+ and K^+, repectively. Similarly, $[Na^+]_i$ and $[K^+]_i$ refer to the intracellular concentrations of Na^+ and K^+. [ATP] is the intracellular concentration of ATP. The meanings and the values of all the rate and equilibrium constants in eqs 5−7 are given in Table 1.

The results of simulations based on model 1 (eqs 1−7) are shown in Figure 2. The starting condition of the simulations was chosen such that all of the enzyme was initially in the E_1 state, that is, $[E_1] = 1$, $[E_2P] = 0$, $[E_2] = 0$. After a short pre-steady-state induction period (generally <1 s), the system reaches a steady state and the inorganic phosphate concentration increases linearly with time. The enzyme turnover number is then given by the value of $d[P_i]/dt$. To compare the results of the simulations with the data reported by Skou (*25*), the turnover numbers have been normalized to a percentage of the maximum activity with optimum Na^+ and K^+ concentrations (Figure 2). Comparison of the simulations with the experimental data shows that, although the sharp drop in activity at high Na^+ and low K^+ concentrations is reasonably well reproduced by the simulations of model 1, the increase in activity at low Na^+ concentrations displayed by the simulations is virtually hyperbolic rather than the experimental sigmoidal behavior. It is thus obvious that this model must still be lacking some important feature or features of the enzyme's kinetic behavior. Skou (*15*, *25*) proposed that the sigmoidal activation of the enzyme by Na^+ may be because more than one Na^+ ion must bind before phosphorylation can occur. Model 1 already incorporates, however, the idea that phosphorylation requires three bound Na^+ ions. It would appear, therefore, that an additional property of the enzyme may be responsible for the marked sigmoidicity experimentally observed.

Model 2: Complete Irreversibility, Na^+/K^+ Competition. Based on numerous experimental studies (*21*, *22*, *32*−*37*), it now seems clear that two of the cytoplasmic transport sites are relatively nonspecific and that Na^+ and K^+ can bind in competition to one another to the E_1 conformation. The third cytoplasmic site appears to be, however, quite specific for Na^+ ions. On the basis of this, it is reasonable to expect that the high K^+ concentrations present at the beginning of the activity curve should suppress the kinetics of the phosphorylation reaction and that this could enhance the sigmoidicity of the curve. In our second kinetic model, we therefore include competition between intracellular Na^+ and K^+ for the first two binding sites on E_1. In this case, all of the equations remain the same as those for model 1, except for eq 6, which requires the addition of further terms to account for the competitive inhibition of phosphorylation by K^+. The new expression for k_2^{obs} then becomes

$$k_2^{obs} = k_2 \frac{[ATP]/K'_A}{1 + [ATP]/K'_A} \times \frac{[Na^+]_i^3/(K_{N1}^2 K_{N2})}{1 + \frac{2[Na^+]_i}{K_{N1}} + \frac{[Na^+]_i^2}{K_{N1}^2} + \frac{[Na^+]_i^3}{(K_{N1}^2 K_{N2})} + \frac{2[Na^+]_i[K^+]_i}{(K_{N1}K_K^i)} + \frac{2[K^+]_i}{K_K^i} + \frac{[K^+]_i^2}{(K_K^i)^2}} \quad (6a)$$

Simulations using model 2 are also shown in Figure 2. The simulated curves are now much more sigmoidal in the low Na^+ concentration range, and the calculated activity has decreased at low Na^+ concentrations in comparison to the results of model 1. The agreement with the experimental data of Skou (*25*) is now much improved (see Figure 2), but the calculated activities are still much too high in the low Na^+ concentration range and the sigmoidicity of the simulated curve is still too low. There must, therefore, be still another

effect of either Na^+ or K^+ ions that is responsible for the sigmoidal behavior.

Model 3: E_2-E_1 Reversibility, Na^+/K^+ Competition. So far both models used have assumed complete irreversibility of all three enzyme reactions. It is well-known, however, that an equilibrium exists between the E_1 and the E_2 conformations, which can be shifted by changing the solution composition (*5*, *35*, *38*−*42*). It is very likely, therefore, that K^+ ions not only compete with Na^+ ions for sites on the E_1 conformation but when they bind they also drive the enzyme back into the E_2 conformation. Direct kinetic evidence for a K^+-stimulated $E_1 \rightarrow E_2$ transition has indeed been found by several groups (*18*, *19*, *35*−*37*, *43*−*45*). In our third model of Na^+,K^+-ATPase kinetics, we have, thus, included the backward reaction, $E_1 \rightarrow E_2$, and an additional rate constant, k_{-1}^{obs}, for this reaction (see Figure 1). The set of differential equations describing this model are as follows:

$$\frac{d[E_1]}{dt} = k_1^{obs}[E_2] - k_2^{obs}[E_1] - k_{-1}^{obs}[E_1] \quad (8)$$

$$\frac{d[E_2P]}{dt} = k_2^{obs}[E_1] - k_4^{obs}[E_2P] \quad (9)$$

$$\frac{d[E_2]}{dt} = k_4^{obs}[E_2P] - k_1^{obs}[E_2] + k_{-1}^{obs}[E_1] \quad (10)$$

$$\frac{d[P_i]}{dt} = k_4^{obs}[E_2P] \quad (11)$$

Again, assuming that Na^+ and K^+ compete for two sites on E_1 and that two K^+ are required to bind to stimulate the $E_1 \rightarrow E_2$ transition, k_{-1}^{obs} is related to the Na^+ and K^+ concentrations by

$$k_{-1}^{obs} = k_{-1}^{a}(1 - A) + k_{-1}^{b}A \quad (12)$$

where

$$A = \frac{[K^+]_i^2/(K_K^i)^2}{\left(1 + \frac{[K^+]_i}{K_K^i}\right)^2 + \frac{2[Na^+]_i}{K_{N1}} + \frac{2[Na^+]_i[K^+]_i}{(K_{N1}K_K^i)} + \frac{[Na^+]_i^2}{K_{N1}^2} + \frac{[Na^+]_i^3}{(K_{N1}K_{N2}^2)}} \quad (13)$$

Simulations using model 3 are also shown in Figure 2. It can be seen that the experimentally observed sigmoidicity at low Na^+ concencentrations is now further enhanced and the overall agreement of the simulated curve with the data of Skou (*25*) is better than that obtained with either model 1 or 2. Differences between the simulated and experimental curves are, however, still apparent. Model 3 appears to increase the sigmoidicity too strongly at low Na^+ concentrations such that the rise in activity is too rapid. Furthermore, all three models predict too steep a drop off in activity at low K^+ and high Na^+ concentrations. This could be explained by Na^+/K^+ competition on the extracellular face of the enzyme in addition to that on the cytoplasmic face. High Na^+ concentrations may in fact inhibit dephosphorylation of the enzyme by competing with K^+ ions and driving the enzyme back into the $E_1P(Na^+)_3$ state (*23*, *46*). To include this effect, the model must be extended by explicitly taking into account the $E_1P \rightarrow E_2P$ transition rather than including it in the phosphorylation reaction.

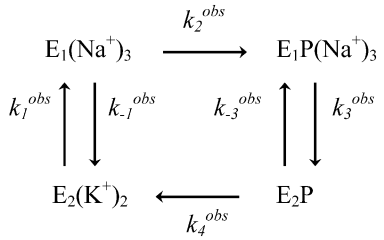

FIGURE 3: Reaction scheme of model 4 showing only those reactions of the Na^+,K^+-ATPase considered to be rate-determining. As for Figure 1, please note that, for simplicity, ATP has not been explicitly included in the reaction scheme. ATP is, however, naturally required for the phosphorylation step ($E_1(Na^+)_3 \rightarrow E_2P(Na^+)_3$), and it can also act on a low-affinity site to accelerate the $E_2(K^+)_2 \rightarrow E_1(Na^+)_3$ transition.

Model 4: E_2-E_1 Reversibility, E_1P-E_2P Reversibility, Na^+/K^+ Competition. In this final model, the reaction scheme has been extended from a three-step cycle to a four-step cycle (see Figure 3). Both the forward ($E_1P \rightarrow E_2P$) and the backward ($E_2P \rightarrow E_1P$) conformational transition of phosphorylated enzyme have been included. The forward reaction, which involves the release of Na^+ ions to the extracellular fluid, is fast and is not a major rate-determining step (*6*). At high extracellular Na^+ concentrations, however, the backward reaction, $E_2P \rightarrow E_1P$, is accelerated, leading to an inhibition of the overall turnover of the enzyme. This effect could at least in part counteract the accelerating effect of extracellular Na^+ ions on the $E_2 \rightarrow E_1$ transition and intracellular K^+ release.

The set of differential rate equations describing model 4 are as follows:

$$\frac{d[E_1]}{dt} = k_1^{obs}[E_2] - k_2^{obs}[E_1] - k_{-1}^{obs}[E_1] \quad (14)$$

$$\frac{d[E_1P]}{dt} = k_2^{obs}[E_1] - k_3^{obs}[E_1P] + k_{-3}^{obs}[E_2P] \quad (15)$$

$$\frac{d[E_2P]}{dt} = k_3^{obs}[E_1P] - k_{-3}^{obs}[E_2P] - k_4^{obs}[E_2P] \quad (16)$$

$$\frac{d[E_2]}{dt} = k_4^{obs}[E_2P] - k_1^{obs}[E_2] + k_{-1}^{obs}[E_1] \quad (17)$$

$$\frac{d[P_i]}{dt} = k_4^{obs}[E_2P] \quad (18)$$

k_3^{obs} is here simply the rate constant for the $E_1P \rightarrow E_2P$ transition, which is assumed only to occur when three Na^+ ions are bound. It has a constant value, independent of any substrate concentrations. At 24 °C and pH 7.4, Babes and Fendler (*46*) determined its value from stationary electrical relaxation measurements to be 225 s^{-1}. From an analysis of measurements at different Na^+ concentrations, they suggested the following expression to explain the dependence of the observed rate constant for the backward $E_2P \rightarrow E_1P$ transition on the extracellular Na^+ concentration:

$$k_{-3}^{obs} = k_{-3}\frac{[Na^+]}{[Na^+] + K_{NP}^o} \quad (19)$$

where K_{NP}^o is the apparent Na^+ dissociation constant of the E_2P conformation (i.e., the Na^+ concentration at which the Na^+ sites are 50% occupied).

In model 4, both the phosphorylation and the dephosphorylation steps are still considered to be irreversible. The justification for these assumptions needs some consideration. Under nonphysiological conditions, it is known that ADP is able to stimulate the reverse of the ATP phosphorylation reaction, which involves the synthesis of ATP, that is, $E_1P + ADP \rightarrow E_1 + ATP$ (*23*). However, under physiological conditions of high excess of ATP over ADP, it is unlikely that this reaction plays a significant role and that the assumption of an irreversible phosphorylation step is justified. Ghosh et al. (*47*) showed, for example, in the case of pancreas cells, that there is a 100-fold excess of ATP over free cytoplasmic ADP. The assumption of an irreversible dephosphorylation also requires some consideration. Phosphorylation of the enzyme by inorganic phosphate in the presence of Mg^{2+} ions has been observed under unphysiological conditions, that is, in the absence of Na^+ and K^+ ions (*48*). In contrast to ADP, the physiological cytoplasmic concentration of inorganic phosphate is considerable. Ghosh et al. (*47*) measured concentrations in the range 3−5 mM, which is in the same range as the ATP concentration. Cornelius et al. (*48*) showed, however, that the rate constant for phosphorylation by inorganic phosphate is at least 100 times slower than that of dephosphorylation in the presence of saturating concentrations of extracellular K^+. Unless one is considering unphysiological conditions of submillimolar extracellular K^+ concentrations, the assumption of an irreversible dephosphorylation step would, therefore, also seem justified.

The results of simulations based on model 4 (eqs 5, 7, 6a, and 12−19) are shown in Figure 2. Although there are still differences between the simulated data and the experimental data of Skou (*25*), the agreement is significantly improved over model 3, particularly at high Na^+ concentrations. The differences that still exist could easily be accounted for by variations in the rate or equilibrium constants of individual reactions due to species differences or to the different temperatures used for the steady-state and the transient kinetic measurements. Since model 4 predicts all the essential features of the activity curve, we shall use it as a basis for discussion of the pump's short-term regulation under physiological conditions.

DISCUSSION

Four mathematical models of the Na^+,K^+-ATPase steady-state activity have been presented. Within each mathematical model, the major rate-determining steps (phosphorylation, dephosphorylation, and the $E_2 \rightarrow E_1$ conformational change) have been described by differential rate equations, which are solved numerically, whereas the faster binding steps of Na^+, K^+, and ATP have been considered to be in equilibrium on the time scale of the rate-determining steps and have hence been described by analytical expressions. By comparison with published experimental data of the enzyme's steady-state activity at varying Na^+ and K^+ concentrations (*25*), it was found that model 4 best explains the enzyme's behavior. This model (see Figure 3) involves irreversible phosphorylation ($E_1 \rightarrow E_1P$) and dephosphorylation ($E_2P \rightarrow E_2$) steps, but reversible conformational changes of unphosphorylated and phosphorylated enzyme ($E_2 \leftrightarrow E_1$ and $E_1P \leftrightarrow E_2P$). Another important feature of the model is competition between Na^+ and K^+ for two of the three cytoplasmic ion binding sites.

Model 4 still does not incorporate many of the reactions of the enzyme observed in vitro under steady-state and pre-steady-state conditions, for example, back-door phosphorylation by inorganic phosphate, ADP-induced dephosphorylation, and *p*-nitrophenylphosphatase activity. Furthermore, it does not take into account the enzyme's pH dependence, voltage dependence, or temperature dependence. Nevertheless, as demonstrated in Figure 2, it does provide estimates of the enzyme's activity and its dependence on intracellular and extracellular concentrations of Na^+, K^+, and ATP. As long as one sticks to conditions close to the physiological case, model 4 then provides a framework for the discussion of the enzyme's regulation in vivo.

Now let us consider the physiological conditions of the enzyme. The normal intracellular Na^+ and K^+ concentrations are 10−20 mM and about 120 mM, respectively. The normal extracellular concentrations are about 4 mM K^+ and 140 mM Na^+ (*15*). The typical intracellular ATP concentration is 1−5 mM, depending on the type of cell (*49*). With the use of these typical concentrations ($[Na^+]_i = 15$ mM, $[Na^+]_o = 140$ mM, $[K^+]_i = 120$ mM, $[K^+]_o = 4$ mM, $[ATP] = 3$ mM), it is possible to calculate from the models the expected turnover number of the enzyme at physiological concentrations. For models 1, 2, 3, and 4 this yields values of 34, 14, 3.9, and 3.8 s^{-1}. The lower values calculated for models 2, 3, and 4 are due to the inhibitory effect of the high internal K^+ concentration, which has been assumed to compete with intracellular Na^+ in model 2 and furthermore to accelerate the back reaction from E_1 to E_2 in models 3 and 4. Each of the values refers to a temperature of around 24 °C, since this was the temperature used in the determination of the majority of the rate constants used in the models (see Table 1). At 37 °C, the turnover numbers would be expected to be significantly higher.

The 100% values at optimum Na^+ and K^+ concentrations for each model correspond to turnover numbers of 38 s^{-1} (models 1−3) and 31 s^{-1} (model 4). Again these values all refer to a temperature of around 24 °C. Comparing these maximum turnovers to those given above for physiological concentrations, we can calculate the percentages of maximal activity of the enzyme to be 91%, 38%, 10%, or 12% according to model 1, 2, 3, or 4, respectively. The final value, calculated with the most complete model, agrees well with that of 10−15% reported by Skou (*50*). It is, thus, clear, as Skou already pointed out, that the enzyme has under physiological conditions a large reserve power and is hence capable of acute regulation at the molecular level, for example, automatically by changes in substrate concentrations or via changes in its kinetic or equilibrium constants.

With use of the kinetic model 4 presented here, it is now possible to investigate likely modes of regulation of the enzyme. To identify the most likely potential mechanisms of regulation, the tactic we have followed has been to independently vary the physiological concentrations of Na^+,

Table 2: Effects of ±10% Variations in the Substrate Concentrations and Rate and Equilibrium Constants on the Turnover Number of the Enzyme[a]

parameter varied	percentage changes in turnover	
	+10%	−10%
$[Na^+]_i$	+33.2	−27.9
$[Na^+]_o$	+0.99	−1.20
$[K^+]_i$	−17.3	+22.6
$[K^+]_o$	+0.11	−0.15
$[ATP]_i$	+0.17	−0.22
k_1^d	+7.33	−7.66
k_{-1}^b	−6.61	+7.64
k_2	+8.81	−9.02
K_A	−0.18	+0.18
K'_A	−0.026	+0.022
K_N^o	−1.13	+1.16
K_{N1}	−15.6	+19.8
K_{N2}	−11.6	+15.0
K_K^i	+20.3	−18.9

[a] All calculations have been based on model 4, that is, including Na^+/K^+ competition for two of the cytoplasmic ion binding sites and reversibility of the $E_2 \rightarrow E_1$ and $E_1P \rightarrow E_2P$ transitions. The percentage changes in turnover are relative to a value of 3.83 s^{-1}, which was calculated using physiological substrate concentrations of $[Na^+]_i = 15$ mM, $[Na^+]_o = 140$ mM, $[K^+]_i = 120$ mM, $[K^+]_o = 4$ mM, and $[ATP]_i = 3$ mM and the values of the rate and equilibrium constants given in Table 1. The values of the parameters k_1^a, k_1^b, k_1^c, k_{-1}^a, k_3, k_{-3}, k_4^a, k_4^b, K_{NP}^o, K_{K1}^o, and K_{K2}^o were also varied by ±10%, but their effects on the turnover were all found to be less than 1%.

K^+, and ATP, as well as all of the rate constants and equilibrium constants included in the model. We then determined the percentage change in turnover produced by the change in each parameter. The results of these calculations are shown in Table 2.

The calculations show that the enzyme turnover is relatively insensitive to changes in the extracellular Na^+ and K^+ concentrations and the intracellular ATP concentration. This is because the physiological concentrations of these substrates generally already far exceed their relevant dissociation constants, so the enzyme's binding sites are very close to being saturated in each case. In contrast, the turnover is very sensitive to changes in the intracellular concentrations of Na^+ and K^+. Changes in their concentrations by 10% yield turnover number changes of between 17% and 33%. Changes in the intracellular Na^+ and K^+ concentrations are, therefore, a very likely mechanism of direct self-regulation of the enzyme. The strong dependence on intracellular Na^+ and K^+ can be explained by their competition at cytoplasmic sites of the enzyme and by their inhibition (in the case of Na^+) and stimulation (in the case of K^+) of the reverse reaction of the enzyme, $E_1 \rightarrow E_2$.

If one inspects the dependence of the turnover shown in Table 2 on the values of the rate constants, it can easily be seen that the enzyme is most sensitive to the values of k_1^d, k_{-1}^b, and k_2. Ten percent changes in the values of these rate constants yield changes in the turnover number of between 6.6% and 9.0%. In comparison, the turnover shows negligible dependence on the values of all other rate constants. The dependence on k_1^d can easily be understood, since it is the rate constant for the $E_2 \rightarrow E_1$ transition under conditions of saturating extracellular Na^+ and intracellular ATP, which has been shown to be the major rate-determining step of the enzyme cycle (*5*). The dependence on k_{-1}^b (the rate constant for the reverse reaction $E_1 \rightarrow E_2$ under saturating intracellular K^+ concentrations) can also be easily understood, because an increase in its value has a direct inhibitory effect on the overall rate-determining conversion of enzyme from the E_2 state into the E_1 state. The relatively strong dependence of the turnover on the value of k_2 (the rate constant for ATP phosphorylation under saturating intracellular Na^+ concentrations) is perhaps somewhat surprising considering that the phosphorylation reaction is more than twice as fast as the $E_2 \rightarrow E_1$ conformational change (i.e., the value of $k_2 = 180$ s^{-1} whereas that of $k_1^d = 70$ s^{-1}). However, at the physiological intracellular concentrations of Na^+ and K^+, the cytoplasmic ion binding sites are far from saturated by Na^+ and hence the observed rate constant for ATP phosphorylation, k_2^{obs}, is far less than its maximum value of 180 s^{-1}. Using eq 6a, one can calculate that the value of k_2^{obs} under physiological conditions should only be approximately 21 s^{-1}. For comparison, at the same substrate concentrations, the observed rate constant for the $E_2 \rightarrow E_1$ transition, k_1^{obs}, can be calculated from eq 5 to be 58 s^{-1}. Under physiological conditions, therefore, both the $E_2 \rightarrow E_1$ transition and the phosphorylation of the enzyme by ATP are important rate-determining steps of the cycle and hence any changes in their maximum rate constants is a likely mechanism for regulation of the enzyme's steady-state activity.

Now looking at the effects of changing the enzyme's dissociation constants for its various substrates, one can easily see that the turnover number is most strongly affected by changes in its dissociation constants for intracellular Na^+, K_{N1} and K_{N2}, and intracellular K^+, K_K^i. Ten percent changes in these parameters cause changes in turnover number of between 12% and 20% (see Table 2). By comparison, changes caused by variations in any of the other dissociation constants are relatively insignificant. The dependence of the turnover number on K_{N1}, K_{N2}, and K_K^i can be explained by the competition of Na^+ and K^+ for cytoplasmic binding sites on the enzyme and their effects on the rate of ATP phosphorylation and the $E_1 \rightarrow E_2$ conformational transition. From eq 6a, it can be shown that under physiological conditions the Na^+ sites necessary for phosphorylation are only approximately 12% saturated. Any decrease in the Na^+ dissociation constants, K_{N1} and K_{N2}, would therefore lead to an increase in the occupancy of the cytoplasmic Na^+ sites and a consequent increase in the observed rate constant for phosphorylation, k_2^{obs}, and hence in the overall turnover. Similarly, an increase in the microscopic dissociation constant for K^+ will lead to decreased competition from K^+ for the cytoplasmic sites, resulting in a greater occupancy by Na^+ and hence a higher value of k_2^{obs} and the turnover number. The competition between Na^+ and K^+ also affects the degree of inhibition of the enzyme's turnover via the $E_1 \rightarrow E_2$ conformational transition (cf. eqs 12 and 13). Decreases in the Na^+ dissociation constants, K_{N1} and K_{N2}, will hinder the occupation of the cytoplasmic sites by K^+ and hence reduce the observed rate constant of the K^+-stimulated $E_1 \rightarrow E_2$ transition, k_{-1}^{obs}, thus enhancing the enzyme's turnover in the forward direction. A decrease in the K^+ microscopic dissociation constant, K_K^i, would enhance the observed rate constant of the K^+-stimulated $E_1 \rightarrow E_2$ transition, leading to inhibition of the enzyme's turnover number. Based on the

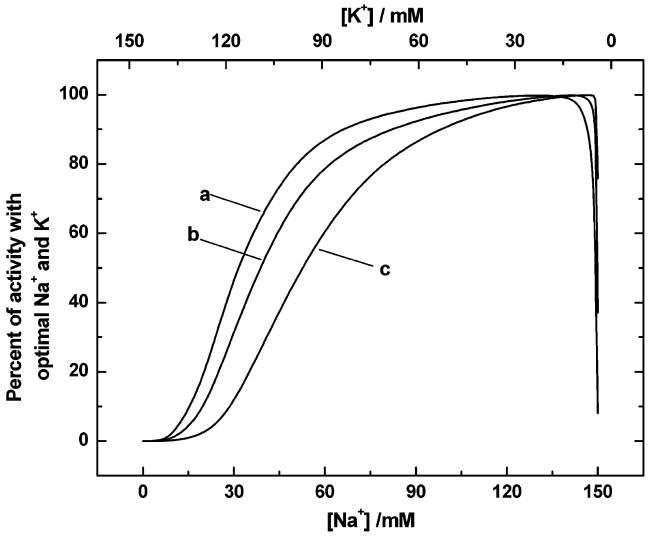

FIGURE 4: Simulations of the effect of Na^+ and K^+ ($Na^+ + K^+ = 150$ mM) on the catalytic activity of the Na^+,K^+-ATPase at cytoplasmic ATP concentrations of 3 mM (curve a), 10 μM (curve b), and 1 μM (curve c). For each curve, the 100% of optimum activity values correspond to turnover numbers of 30.9 s^{-1} (3 mM ATP), 6.56 s^{-1} (10 μM ATP), and 1.34 s^{-1} (1 μM ATP).

calculations shown in Table 2, therefore, changes in the affinities of the cytoplasmic binding sites for Na^+ and K^+ are very likely mechanisms of Na^+,K^+-ATPase regulation.

Up to now we have been considering the most common physiological conditions under which the Na^+,K^+-ATPase operates. Significant variations in physiological conditions can, however, occur in different tissues of the body. One particularly interesting case is in the kidney, where the Na^+,K^+-ATPase forms the Na^+ concentration gradient necessary for the reabsorption of nutrients into the bloodstream. Blood flow to different parts of the kidney is known to vary significantly (*51*). Blood flow to the cortex, where glomerular filtration occurs, is approximately twice that of the outer medulla. As a consequence, the partial pressure of oxygen in the outer medulla, where the Na^+,K^+-ATPase is found in particularly high concentrations, is up to five times lower than that found in the cortex, that is, ~10−20 mmHg in the outer medulla compared to ~50 mmHg in the cortex. Since the oxygen supply to the outer medulla is so low, the amount of ATP produced in the cell cytoplasm is also expected to be much lower than normal. To consider this particular situation, we have, therefore, carried out a series of simulations of Napoleon's hat curves using model 4 at decreasing ATP concentrations (see Figure 4). It can be seen that once the ATP concentration decreases into the micromolar range, there is a significant decrease in the steepness of the increase in activity and a shift of the half-maximal activity to higher Na^+ concentrations (or lower K^+ concentrations). This behavior agrees qualitatively with that found experimentally by Skou (*26*), who carried out experiments at ATP concentrations of 3 mM and 0.1 μM. Unfortunately a direct comparison of the simulations with Skou's data is not possible in this case, because at an ATP concentration of 0.1 μM it can be calculated from published data on the kinetics of ATP binding (*52*) that the pseudo-first-order rate constant for ATP binding would be expected to be only around 3 s^{-1}. Under these conditions, the ATP binding reaction would have to be considered as a significant rate-determining step and the assumption of the model of an ATP binding equilibrium would break down. At an ATP concentration of 1 μM, however, we have carried out simulations of the steady-state activity to determine whether under these conditions other possible sites of regulation might become active. The Na^+ and K^+ concentrations used for the simulations were as in the previous ones (i.e., $[Na^+]_i = 15$ mM, $[Na^+]_o = 140$ mM, $[K^+]_i = 120$ mM, $[K^+]_o = 4$ mM). In this case, it was found that 10% positive and negative variation in the cytoplasmic ATP concentration caused a change in activity of +14.6% and −13.8%, respectively. Similar variations in the high-affinity ATP site's dissociation constant (K'_A) caused changes of −8.1% and +9.7%. If one varies the low-affinity ATP site's dissociation constant (K_A), the changes are −4.9% and +6.0%. Under conditions of low blood flow and low ATP concentrations (micromolar range), as could occur in the kidney, it can, thus, be seen that the enzyme's activity becomes much more sensitive to variations in the cytoplasmic ATP concentrations and in its ATP dissociation constants. These could then become additional possible sites of regulation under such conditions.

When the in vivo hormonal regulation of the Na^+,K^+-ATPase is discussed, three levels of regulation are generally considered (*53*). Sustained long-term changes in pump activity can come about via changes in gene expression, resulting in an increase or a decrease in the total number of available pump units in the membrane. A second level of regulation has been proposed involving the translocation of pump units from intracellular storage compartments to the plasma membrane. In this paper, we have concentrated on acute short-term regulation in pump activity, which occurs at the level of individual pump units and involves a change in the steady-state activity of each affected pump molecule. Summarizing the results given in Table 2 reveals the major effects that could lead to short-term regulation involve changes in the cytoplasmic Na^+ and K^+ ion concentrations, changes in the cytoplasmic Na^+ and K^+ ion affinities, and changes in the rate constants for phosphorylation, the $E_2 \rightarrow E_1$ conformational change, and the $E_1 \rightarrow E_2$ conformational change. Although it has been found that these are the most sensitive sites in the Na^+,K^+-ATPase pump cycle in determining the overall turnover number and are thus prime candidates for regulation, it must be pointed out, however, that this does not necessarily preclude the participation of other steps of the pump cycle in regulation. If a dramatic change in a rate or equilibrium constant, which under normal conditions has little effect on determining the overall turnover number, occurs, then the step involved could still conceivably be involved in regulation.

The sensitivity of the enzyme's steady-state activity to the cytoplasmic Na^+ and K^+ concentrations allows it to compensate automatically for any fluctuations in cytoplasmic ion concentrations. It could, however, also be involved in hormonal regulation. One proposed mechanism of insulin action on the Na^+,K^+-ATPase (*54*, *55*) suggests that the hormone induces an increase in the cytoplasmic Na^+ concentration, thus leading to an increase in pump activity. Another proposed mechanism of insulin activity is via an increase in cytoplasmic Na^+ affinity of the enzyme (*56*). Both of these proposed mechanisms of insulin action can be considered feasible on the basis of the calculations presented here. Another mechanism of regulation, which has recently

been attracting a great deal of attention, is regulation of the enyzme via phosphorylation by protein kinase A or C. The molecular basis of Na^+,K^+-ATPase regulation by protein kinase phosphorylation is still under discussion. On the basis of the calculations presented here, however, it would seem most likely that the protein kinase phosphorylated enzyme has altered cytoplasmic Na^+ or K^+ affinities or an altered maximum activity (V_{max}) or both, due to changes in its rate constants for ATP phosphorylation or the conformational change of unphosphorylated enzyme (either $E_2 \rightarrow E_1$ or $E_1 \rightarrow E_2$).

Another likely mechanism of Na^+,K^+-ATPase regulation appears to be via protein−protein interactions within the cell membrane, that is, between the catalytic $\alpha\beta$ complex of the enzyme and the γ subunit in the kidney or other members of the FXYD family of small hydrophobic proteins in other tissues (*57*). There now seems to be general agreement that one of the major effects of the γ subunit is to regulate the enzyme by modulating its affinity for Na^+ or K^+ or both (*58*, *59*). This is certainly consistent with the results of the simulations presented here, since the steady-state turnover has been found to be particularly sensitive to changes in the intrinsic dissociation constants of the enzyme for cytoplasmic Na^+ and K^+. There is still disagreement in the literature, however, concerning the details of the mechanisms of γ subunit modulation of Na^+,K^+-ATPase activity. Therien et al. (*58*) suggest that the enzyme's apparent affinity for Na^+ ions on the cytoplasmic surface is reduced by an increase in its intrinsic K^+ affinity, thus resulting in an increase in K^+/Na^+ antagonism. Arystarkhova et al. (*59*) have argued that the enzyme's intrinsic affinity for Na^+ may also be reduced by the γ subunit. As pointed out by Arystarkhova et al. (*59*), one reason that may have contributed to the different interpretations drawn by the two groups could have been the kinetic model used in explaining the results. Therien et al. (*58*) used a model in which K^+ competes noncooperatively for all three Na^+ sites, whereas Arystarkova et al. (*59*) allowed more realistically for the possibility of cooperativity. The model presented here incorporates cooperativity and considers competition between Na^+ and K^+ for two nonspecific sites.

Therien et al. (*58*) also found that the γ subunit increased the enzyme's apparent affinity for ATP. This could be due to a change in the enzyme's intrinsic ATP dissociation constants, K_A and K'_A (to E_2 and E_1, respectively), since at low ATP concentrations in the kidney outer medulla these have been shown here to be possible regulatory sites. This is, however, only likely to be the case if the low oxygen supply to the kidney medulla results in a cytoplasmic ATP concentration in the micromolar range. The change in apparent affinity for ATP could also be a byproduct of a regulatory change in the rate constants for the conformational change of unphosphorylated enzyme, that is, an increase in the rate constant of $E_2Na^+ATP \rightarrow E_1Na^+ATP$ or a decrease in the rate constant of $E_1(K^+)_2 \rightarrow E_2(K^+)_2$ or both, which would lead to a shift in the conformational equilibrium toward E_1. In contrast, however, Arystarkhova et al. (*59*) have reported that the elimination of the γ subunit in γ knock-out animals produces no significant change in ATP affinity. The possibility of a regulatory shift in the E_1/E_2 equilibrium or a change in intrinsic ATP affinity by the γ subunit are thus still open to question.

ACKNOWLEDGMENT

The authors thank Prof. Jens-Christian Skou, Dr. Flemming Cornelius, and Prof. Dr. Hans-Jürgen Apell for helpful discussions, and Dr. Binh Pham for assistance with the diagrams.

REFERENCES

1. Skou, J. C. (1957) The influence of some cations on an adenosine triphosphatase from peripheral nerves, *Biochim. Biophys. Acta 23*, 394−401.
2. Scheiner-Bobis, G. (2002) The sodium pump. Its molecular properties and mechanics of ion transport, *Eur. J. Biochem. 269*, 2424−2433.
3. Heyse, S., Wuddel, I., Apell, H.-J., and Stürmer W. (1994) Partial reactions of the Na, K.-ATPase: determination of rate constants, *J. Gen. Physiol. 104*, 197−240.
4. Apell, H.-J. (1997) Kinetic and energetic aspects of Na^+/K^+-transport cycle steps, *Ann. N. Y. Acad. Sci. 834*, 221−230.
5. Lüpfert, C., Grell, E., Pintschovius, V., Apell, H.-J, Cornelius, F., and Clarke, R. J. (2001) Rate limitation of the Na^+,K^+-ATPase pump cycle, *Biophys. J. 81*, 2069−2081.
6. Bamberg, E., Clarke, R. J., and Fendler, K. (2001) Electrogenic properties of the Na^+,K^+-ATPase probed by presteady state and relaxation studies, *J. Bioenerg. Biomembr. 33*, 401−405.
7. Kane, D. J., Fendler, K., Grell, E., Bamberg, E., Taniguchi, K., Froehlich, J. P., and Clarke, R. J. (1997) Stopped-flow kinetic investigations of conformational changes of pig kidney Na^+,K^+-ATPase, *Biochemistry 36*, 13406−13420.
8. Kane, D. J., Grell, E., Bamberg, E., and Clarke, R. J. (1998) Dephosphorylation kinetics of pig kidney Na^+,K^+-ATPase, *Biochemistry 37*, 4581−4591.
9. Clarke, R. J., Kane, D. J., Apell, H.-J., Roudna, M., and Bamberg, E. (1998) Kinetics of Na^+-dependent conformational changes of rabbit kidney Na^+,K^+-ATPase, *Biophys. J. 75*, 1340−1353.
10. Ganea, C., Babes, A., Lüpfert, C., Grell, E., Fendler, K., and Clarke, R. J. (1999) Hofmeister effects of anions on the kinetics of partial reactions of the Na^+,K^+-ATPase, *Biophys. J. 77*, 267−281.
11. Geibel, S., Barth, A., Amslinger, S., Jung, A. H., Burzik, C., Clarke, R. J., Givens, R. S., and Fendler, K. (2000) P^3-[2-(4-hydroxyphenyl)-2-oxo]ethyl ATP for the rapid activation of the Na^+,K^+-ATPase, *Biophys. J. 79*, 1346−1357.
12. Humphrey, P. A., Lüpfert, C., Apell, H.-J., Cornelius, F., and Clarke, R. J. (2002) Mechanism of the rate-determining step of the Na^+,K^+-ATPase pump cycle, *Biochemistry 41*, 9496−9507.
13. Hansen, P. S., Buhagiar, K. A., Kong, B. Y., Clarke, R. J., Gray, D. F., and Rasmussen, H. H. (2002) Dependence of Na^+-K^+ pump current−voltage relationship on intracellular Na^+, K^+, and Cs^+ in rabbit cardiac myocytes, *Am. J. Physiol. Cell Physiol. 283*, C1511−C1521.
14. Jørgensen, P. L., and Andersen, J. P. (1988) Structural basis for E_1-E_2 conformational transitions in Na,K-pump and Ca-pump proteins, *J. Membr. Biol. 103*, 95−120.
15. Skou, J. C. (1990) The energy coupled exchange of Na^+ for K^+ across the cell membrane. The Na^+,K^+-pump, *FEBS Lett. 268*, 314−324.
16. Cornelius, F. (1991) Functional reconstitution of the sodium pump. Kinetics of exchange reactions performed by reconstituted Na/K-ATPase, *Biochim. Biophys. Acta 1071*, 19−66.
17. Karlish, S. J. D., and Yates, D. W. (1978) Tryptophan fluorescence of ($Na^+ + K^+$)-ATPase as a tool for study of the enzyme mechanism, *Biochim. Biophys. Acta 527*, 115−130.
18. Steinberg, M, and Karlish, S. J. D. (1989) Studies on conformational changes in Na,K-ATPase labeled with 5-iodoacetamidofluorescein, *J. Biol. Chem. 264*, 2726−2734.
19. Pratap, P. R., Palit, A., Grassi-Nemeth, E., and Robinson, J. D. (1996) Kinetics of conformational changes associated with potassium binding to and release from Na^+/K^+-ATPase, *Biochim. Biophys. Acta 1285*, 203-211.
20. Forbush, B., III. (1987) Rapid release of ^{42}K and ^{86}Rb from an occluded state of the Na,K-pump in the presence of ATP or ADP, *J. Biol. Chem. 262*, 11104−11115.
21. van der Hijden, H. T. W. M., and de Pont, J. J. H. H. M. (1989) Cation sidedness in the phosphorylation step of Na^+/K^+-ATPase, *Biochim. Biophys. Acta 983*, 142−152.

22. Hasenauer, J., Huang W.-H., and Askari, A. (1993) Allosteric regulation of the access channels to the Rb^+ occlusion sites of ($Na^+ + K^+$)-ATPase, *J. Biol. Chem. 268*, 3289−3297.
23. Taniguchi, K., and Post, R. L. (1975) Synthesis of adenosine triphosphate and exchange between inorganic phosphate and adenosine triphosphate in sodium and potassium ion transport adenosine triphosphatase, *J. Biol. Chem. 250*, 3010−3018.
24. Skou, J. C. (1962) Preparation from mammalian brain and kidney of the enzyme system involved in active transport of Na^+ and K^+, *Biochim. Biophys. Acta 58*, 314−325.
25. Skou, J. C. (1975) The ($Na^+ + K^+$) activated enzyme system and its relationship to transport of sodium and potassium, *Q. Rev. Biophys. 7*, 401−434.
26. Skou, J. C. (1979) Effects of ATP on the intermediary steps of the reaction of the ($Na^+ + K^+$)-ATPase. IV. Effect of ATP on $K_{0.5}$ for Na^+ and on hydrolysis at different pH and temperature, *Biochim. Biophys. Acta 567*, 421−435.
27. Sweadner, K. J. (1989) Isozymes of the Na^+/K^+-ATPase, *Biochim. Biophys. Acta 988*, 185−220.
28. Eigen, M. (1968) New looks and outlooks on physical enzymology, *Q. Rev. Biophys. 1*, 3−33.
29. Kirschner, K., Eigen, M., Bittman, R., and Voigt, B. (1966) The binding of nicotinamide-adenine dinucleotide to yeast d-glyceraldehyde-3-phosphate dehydrogenase: Temperature-jump relaxation studies on the mechanism of an allosteric enzyme, *Proc. Natl. Acad. Sci. U.S.A. 56*, 1661−1667.
30. Kirschner, K., Gallego, E., Schuster, I., and Goodall, D. (1971) Cooperative binding of nicotinamide-adenine dinucleotide to years glyceraldehyde-3-phosphate dehydrogenase. I. Equilibrium and temperature-jump studies at pH 8.5 and 40 °C, *J. Mol. Biol. 58*, 29−50.
31. Kirschner, K. (1971) Cooperative binding of nicotinamide-adenine dinucleotide to yeast glyceraldehyde-3-phosphate dehydrogenase. II. Stopped-flow studies at pH 8.5 and 40 °C, *J. Mol. Biol. 58*, 51−68.
32. Garay, R. P., and Garrahan, P. J. (1973) The interaction of sodium and potassium with the sodium pump in red cells, *J. Physiol. 231*, 297−325.
33. Sachs, J. R. (1986) The order of addition of sodium and release of potassium at the inside of the sodium pump of the human red cell, *J. Physiol. 381*, 149−168.
34. Cornelius, F. (1992) *Cis*-allosteric effects of cytoplasmic Na^+/K^+ discrimination at varying pH. Low-affinity multisite inhibition of cytoplasmic K^+ in reconsitituted Na^+/K^+-ATPase engaged in uncoupled Na^+-efflux, *Biochim. Biophys. Acta 1108*, 190−200.
35. Karlish, S. J. D. (1980) Characterization of conformational changes in (Na,K)ATPase labeled with fluorescein at the active site, *J. Bioenerg. Biomembr. 12*, 111−136.
36. Faller, L. D., Diaz, R. A., Scheiner-Bobis, G., and Farley, R. A. (1991) Temperature dependence of the rates of conformational changes reported by fluorescein 5′-isothiocyanate modification of H^+,K^+- and Na^+,K^+-ATPases, *Biochemistry 30*, 3503−3510.
37. Smirnova, I. N., Lin, S.-H., and Faller, L. D. (1995) An equivalent site mechanism for Na^+ and K^+ binding to sodium pump and control of the conformational change reported by fluorescein 5′-isothiocyanate modification, *Biochemistry 34*, 8657−8667.
38. Matsui, H., and Homareda, H. (1982) Interaction of sodium and potassium ions with Na^+,K^+-ATPase. Ouabain-sensitive alternative binding of three Na^+ or two K^+ ions to the enzyme, *J. Biochem. 92*, 193−217.
39. Skou, J. C., and Esmann, M. (1983) The effects of Na^+ and K^+ on the conformational transitions of ($Na^+ + K^+$)-ATPase, *Biochim. Biophys. Acta 746*, 101−113.
40. Schuurmans Stekhoven, F. M. A. H., Swarts, H. G. P., de Pont, J. J. H. H. M., and Bonting, S. L. (1985) Na^+-like effect of imidazole on the phosphorylation of ($Na^+ + K^+$)-ATPase, *Biochim. Biophys. Acta 815*, 16−24.
41. Schuurmans Stekhoven, F. M. A. H., Swarts, H. G. P., 't Lam, G. K., Zou, Y. S., and de Pont, J. J. H. H. M. (1988) Phosphorylation of ($Na^+ + K^+$)-ATPase; stimulation and inhibition by substituted and unsubstituted amines, *Biochim. Biophys. Acta 937*, 161−176.
42. Grell, E., Warmuth, R., Lewitzki, E., and Ruf, H. (1991) Precision titrations to determine affinity and stoichiometry of alkali, alkaline earth, and buffer cation binding to Na,K-ATPase, in *The Sodium Pump: Recent Developments* (Kaplan, J. H., and De Weer, P., Eds.) pp 441−445, Rockefeller University Press, New York.
43. Smirnova, I. N., and Faller, L. D. (1993) Mechanism of K^+ interaction with fluorescein 5′-isothiocyanate-modified Na^+,K^+-ATPase, *J. Biol. Chem. 268*, 16120−16123.
44. Doludda, M., Lewitzki, E., Ruf, H., and Grell, E. (1994) Kinetics and mechanism of cation-binding to Na^+,K^+-ATPase, in *The Sodium Pump: Structure Mechanism, Hormonal Control and Its Role in Disease* (Bamberg, E., and Schoner, W., Eds.) pp 629−632, Steinkopff Verlag, Darmstadt, Germany.
45. Bugnon, P., Doludda, M., Grell, E., and Merbach, A. E. (1997) High-pressure stopped-flow spectrometer for kinetic studies of fast bioinorganic reactions by absorbance and fluorescence detection, in *High-Pressure Research in the Biosciences and Biotechnology* (Heremans, K., Ed.) pp 143−146, Leuven University Press, Leuven, Belgium.
46. Babes, A., and Fendler, K. (2000) Na^+ transport, and the E_1P−E_2P conformational transition of the Na^+/K^+-ATPase, *Biophys. J. 79*, 2557−2571.
47. Ghosh, A., Ronner, P., Cheong, E., Khalid, P., and Matschinsky, F. M. (1991) The role of ATP and free ADP in metabolic coupling during fuel-stimulated insulin release from islet β-cells in the isolated perfused rat pancreas, *J. Biol. Chem. 34*, 22887−22892.
48. Cornelius, F., Fedosova, N. A., and I. Klodos, I. (1998) E_2P phosphoforms of Na,K-ATPase. II. Interaction of substrate and cation-binding sites in P_i phosphorylation of Na,K-ATPase, *Biochemistry 37*, 16686−16696.
49. Gribble, F. M., Loussouarn, G., Tucker, S. J., Zhao, C., Nichols, C. G., and Ashcroft, F. M. (2000) A novel method for measurement of submembrane ATP concentration, *J. Biol. Chem. 39*, 30046−30049.
50. Skou, J. C. (1992) The Na−K pump, *News Physiol. Sci. 7*, 95−100.
51. Brezis, M., and Rosen, S. (1995) Hypoxia of the renal medulla − Its implications for disease, *N. Engl. J. Med. 332*, 647−655.
52. Esmann, M. (1992) Determination of rate constants for nucleotide dissociation from Na,K-ATPase, *Biochim. Biophys. Acta 1110*, 20−28.
53. Ewart, H. S., and Klip, A. (1995) Hormonal regulation of the Na^+-K^+-ATPase: mechanisms underlying rapid and sustained changes in pump activity, *Am. J. Physiol. 269*, C295−C311.
54. Fehlmann, M., and Freychet, P. (1981) Insulin and glucagon stimulation of (Na^+-K^+)-ATPase transport activity in isolated rat hepatocytes, *J. Biol. Chem. 256*, 7449−7453.
55. Rosic, N. K., Standaert, M. L., and Pollet, R. J. (1985) The mechanism of insulin stimulation of (Na^+,K^+)-ATPase transport activity in muscle, *J. Biol. Chem. 260*, 6206−6212.
56. McGill, D. L., and Guidotti, G. (1991) Insulin stimulates both the α1 and α2 isoforms of the rat adipocyte (Na^+,K^+)ATPase, *J. Biol. Chem. 266*, 15824−15831.
57. Cornelius, F., and Mahmmoud, Y. (2003) Functional modulation of the sodium pump: The regulatory proteins "fixit", *News Physiol. Sci. 18*, 119−124.
58. Therien, A. G., Pu, H. X., Karlish, S. J. D., and Blostein, R. (2001) Molecular and functional studies of the gamma subunit of the sodium pump, *J. Bioenerg. Biomembr. 33*, 407−414.
59. Arystarkhova, E., Donnet, C., Asinovski, N. K., and Sweadner, K. (2002) Differential regulation of renal Na,K-ATPase by splice variants of the γ subunit, *J. Biol. Chem. 277*, 10162−10172.
60. Apell, H.-J., Roudna, M., Corrie, J. E. T., and D. R. Trentham, D. R. (1996) Kinetics of the phosphorylation of Na,K-ATPase by inorganic phosphate detected by a fluorescence method, *Biochemistry 35*, 10922−10930.
61. Hobbs, A. S., Albers, R. W., and J. P. Froehlich, J. P. (1980) Potassium-induced changes in phosphorylation and dephosphorylation of ($Na^+ + K^+$)-ATPase observed in the transient state, *J. Biol. Chem. 255*, 3395−3402.
62. Therien, A. G., and Blostein, R. (1999) K^+/Na^+ antagonism at cytoplasmic sites of Na^+-K^+-ATPase: a tissue-specific mechanism of sodium pump regulation, *Am. J. Physiol. Cell Physiol. 277*, C891−C898.

BI0355443